Scanning Microscopy

Volume 5 | Number 3 Article 8

7-30-1991

Prerequisites of High Resolution Scanning Electron Microscopy

René Hermann
Institute for Cell Biology

Martin Müller
Institute for Cell Biology

Scanning Microscopy, Vol. 5, No. 3, 1991 (Pages 653-664) 0891-7035/91$3.00+.00
Scanning Microscopy International, Chicago (AMF O'Hare), IL 60666 USA

PREREQUISITES OF HIGH RESOLUTION SCANNING ELECTRON MICROSCOPY

René Hermann and Martin Müller*

Laboratory for Electron Microscopy I, ETH Zentrum, Institute for Cell Biology, Schmelzbergstr. 7, CH-8092 Zürich, Switzerland

(Received for publication April 5, 1991, and in revised form July 30, 1991)

Abstract

Cryotechniques must be employed throughout all preparation and observation steps in order to extract high resolution scanning electron microscopical information from biological material.

Cryoimmobilization, followed by freeze-drying and metal-shadowing at low temperature, yields optimal structural information of T4 polyheads used as a test specimen. Freeze-substitution of frozen T4 polyheads and subsequent freeze-drying renders the substructures recognizable but less crisp than freeze-drying from aequous solutions. Critical point drying of ethanol dehydrated chemically fixed, or freeze-substituted test specimens results in complete loss of discrete polyhead structure.

In-lens field-emission scanning electron microscopes and highly sensitive electron detectors are instrumental prerequisites in achieving transmission electron microscope-like resolution of structural details. Shape and size of fine structures, of the test specimen, are accurately imaged at high acceleration voltage (> 7 kV). Precise localization of antigenic sites via ultrasmall (0.8 nm) colloidal gold marker systems by backscattered electrons also depends on the appropriate choice of acceleration voltage.

Contamination of the specimen surface is a serious problem in high resolution scanning electron microscopy. It can be controlled in practice, by photographing selected areas of cooled specimens during the first scan of the electron beam.

Key words: chemical fixation, chromium, colloidal gold, contamination, cryomethods, Fab fragments, high-resolution scanning electron microscopy, platinum/carbon, T4 polyheads.

*Address for correspondence:
Martin Müller, Laboratory for Electron Microscopy I, ETH Zentrum, Schmelzbergstr. 7
CH-8092 Zürich, Switzerland,
Phone No: 0041-1-256 39 39,
Fax No: 0041-1-252 96 13

Introduction

High resolution scanning electron microscopy (SEM) can contribute a great deal to the understanding of events occurring on biological surfaces, even at a molecular level, provided that significant structural elements, down to dimensions of 2 - 4 nm, are preserved as a function of the physiological state. Specimen preparation, signal generation and signal detection, and modern instrumentation have to be interactively optimized with a minimum of compromises to finally reach this goal.

The immobilization of biological material, kept under controlled physiological conditions, is the first and most critical step when attempting to preserve the complex interactions of organells, macromolecules, ions and water near native state. Immobilization must be sufficiently rapid to provide adequate time resolution of the dynamic cellular processes.

Immobilization techniques based on chemical fixation approach their limits. Chemical fixation proceeds very slowly and most of the diffusible ions are lost or redistributed during chemical sample fixation (Coetzee and Van der Merwe, 1984). Altered diffusion properties of membranes result in distortions of shape, volume, and content of the cell, and its components. Additional artifacts are introduced by the preparation steps following chemical fixation (Lee, 1984). Dehydration of chemically fixed samples through a graded series of organic solvents extracts important surface components e.g. glycoproteins (Walther et al., 1984). Drying results in further anisotropic shrinkage.

Cryoimmobilization stops physiological processes very rapidly, permitting high resolution of dynamic cellular events (Knoll et al., 1987; Knoll and Plattner, 1989; Hülser et al., 1989). High cooling rates are required to prevent specimen damage by the formation and growth of ice crystals. There are several rapid freezing techniques which adequately immobilize biological structures up to a thickness of approx. 10 to 20 μm with cooling rates from 10^4 to 10^6 K/sec.

Thicker biological systems up to 500 µm, can be immobilized by high pressure freezing (Müller and Moor, 1984; Moor, 1987). High yields of adequately immobilized material can be attained by optimizing the transfer of pressure and cold to the specimen (Studer et al., 1989; Kiss et al., 1990).

Freeze-drying allows one to control the rate and degree of dehydration (MacKenzie, 1972). Freeze-drying should be performed from clean solvents, e.g. distilled water, in order to avoid the deposition of solutes onto the specimen surface during drying (Miller et al., 1983). Aldehyde prefixation is therefore frequently required to stabilize osmotically sensitive specimens prior to washing with distilled water. Freeze-substitution followed by critical point drying may circumvent problems of chemical fixation at ambient temperature (Barlow and Sleigh, 1979; Baba and Osumi, 1987; Walther et al., 1988). Freeze-substitution followed by freeze-drying from organic solvents was introduced for high voltage TEM studies of cultured cells (Bridgman and Reese, 1984).

Fully or partially hydrated specimens can be observed at low temperatures in SEM's equipped with cryo-attachments (Beckett and Read, 1986; Walther et al., 1990; Read and Jeffree, 1991). Even the most sophisticated cryoattachments, attached to conventional field-emission SEM's do not yield sufficiently detailed information. The components of in-lens field-emission scanning electron microscopes (object stage, cryo-holder) however, permit observation of partially freeze-dried samples with transmission electron microscope-like structural resolution (Hermann and Müller, 1991).

Uncoated biological samples yield low lateral resolution in the SEM due to their large electron interaction volume (Joy, 1984). The electron signal can be accurately localized at the surface by metal coating. The metal film must be thin enough to prevent levelling of underlying surface structures and as fine grained as possible (Peters, 1982). The grain size of condensed metal atoms also depends on the kinetic energy of the evaporated metal atoms. Too high energies, as in the case of high energy ion-beam coating may decompose structures of molecular dimensions (2 - 4 nm). The metal grain size is generally reduced with lower specimen temperatures (Gross et al., 1985). Low specimen temperatures during coating are therefore necessary for both, fine-grained coating layers and for optimal structural preservation through controlled dehydration (MacKenzie, 1972).

Chromium coatings provide a well-localized SE I signal (Peters, 1986) and generally yield excellent high resolution secondary electron (SE) images with metal films of optimal thickness (Hermann et al., 1988). Cooled specimens can be chromium coated by planar magnetron sputtering and electron beam shadowing using double-axis rotary shadowing (DARS; Hermann and Müller, 1991). Equally good structural resolution is obtained after unidirectional platinum/carbon shadowing of cooled, freeze-dried samples, imaged by backscattered electrons (BSE's; Autrata et al., 1986 (SEM study of freeze-fractured TEM replicas); Walther and Hentschel, 1989; Hermann and Müller, 1991).

In-lens field-emission scanning electron microscopes provide an electron beam diameter of less than 1 nm at high acceleration voltage. The electron beam diameter increases with reduced acceleration voltage (4 nm at 1 kV in the Hitachi S-900 HRSEM; Nagatani et al., 1987). At lower acceleration voltage, more energy of the primary electron beam is confined within the SE escape zone, increasing the SE yield. The Hitachi S-900H, a dedicated low voltage HRSEM, permits work at low acceleration voltages with slightly reduced beam diameters (3 nm at 1 kV; Sato et al.,1990). The microscope is difficult to equip with an annular BSE detector due to its narrow polepiece gap. Highly efficient BSE detection may be essential for the unambiguous localization of ultra-small colloidal gold in immunolabelling studies.

Contamination of the specimen surface is a serious problem, especially at the magnifications (> 100'000 x) required for high resolution surface imaging at molecular dimensions (Fourie, 1976; Hren, 1979). The major source of contamination is the specimen itself; contaminants are released from the specimen as a consequence of radiation damage (Engel, 1981) and spread over the scanned area by surface diffusion (Wall, 1980). Cooling the specimen reduces mass loss as well as surface diffusion. In this paper we stress the importance of cryomethods during both specimen preparation and subsequent observation in the scanning electron microscope.

T4 polyheads adsorbed onto thin carbon-foils (reducing sub-surface informations) serve as a test specimen. Their structure is well documented in TEM studies, image reconstruction, and previous SEM experiments (Finch et al., 1964; DeRosier and Klug, 1972; Kistler et al., 1978; Buhle et al., 1985; Hermann and Müller, 1991). T4 polyheads are structurally aberrant mutants of T4 phages (defect in gene 20). The capsomeres of the T4 phage head are arranged in long tubes with a diameter of 86 nm exhibiting a plane, hexagonal lattice structure. The center to center spacing is 13 nm. Capsomeres have a diameter of 8.3 nm and are composed of 6 subunits with a diameter of 3 nm (Laemmli et al., 1976).

The immunological localization of surface antigens, receptors and lectin binding sites, with colloidal gold markers is an important application of high resolution SEM (large colloidal gold particles see Hodges et al., 1987; 5 - 15 nm colloidal gold see Müller et al., 1989).

Colloidal gold particles > 15 nm can be identified with the SE signal (Horisberger and Rosset, 1977). BSE imaging is necessary, however, for accurate localization of smaller colloidal gold (Walther et al., 1983; Walther and Müller, 1986); in the SE image small gold is not discernable from surface details or contaminants. Sub-molecular mapping with ultra-small marker systems can be performed with SEM, if the shape and size of biological fine structures are clearly imaged. The importance of choosing the right acceleration voltage is seen in the study of DARS chromium coated T4 polyheads and Fab fragments coupled to 0.8 nm colloidal gold, adsorbed onto a thin carbon-foil.

Material and Methods

Test specimens

T4 polyheads: T4 polyheads were used to study the influence of preparation techniques on the preservation of structural details in TEM (techniques based on chemical fixation were compared with cryotechniques).

T4 polyheads and unbound gold marked Fab fragments were used to evaluate the effect of instrumental parameters on structural resolution in SEM. Specimens were rapidly frozen, freeze-dried and chromium coated for this study.

Fab fragments coupled to 0.8 nm colloidal gold: Fab fragments of polyclonal rabbit IgG (against T even phage tail fibre proteins) have been prepared by papain digestion according to Porter (1959). The Fab fragments have been coupled to 0.8 nm colloidal gold by Aurion (Wageningen, the Netherlands). Colloidal gold marked Fab fragments were stored in phosphate-buffered salt solution (PBS) without any stabilizing proteins.

Specimen preparation techniques

T4 polyheads were mixed in suspension with colloidal gold approx. 5 nm in diameter (Slot and Geuze, 1985); the gold facilitates focussing and astigmatism correction. T4 polyheads and Fab fragments have been adsorbed onto hydrophilized carbon film supported on a copper grid.

Freeze-drying from aqueous solutions: Specimens were washed in bidistilled water and then cryoimmobilized by plunging into liquid ethane. The samples were subsequently freeze-dried for 1 hour at -85° C at a pressure < 5 x 10^{-7} mbar in a BAF 300 freeze-etch device (Balzers, FL).

Freeze-substitution followed by freeze-drying: Specimens were washed in bidistilled water, then cryoimmobilized by plunging into liquid ethane. Freeze-substitution of T4 polyheads was carried out in anhydrous acetone containing 2% osmium tetroxide. The samples were kept in the freeze-substitution medium at -90° C, -60° C and -30° C for 8 hours in each step (Müller et al., 1980). The samples were then washed in anhydrous acetone at -30° C and re-frozen by plunging into liquid ethane. Samples were then freeze-dried from pure acetone in a BAF 300 (Balzers, FL). After 1 hour at -100° C the temperature was increased to -85° C for an hour prior to metal coating.

Freeze-substitution followed by critical point drying: Specimens were washed in bidistilled water, then cryoimmobilized by plunging into liquid ethane. Freeze-substitution was carried out in anhydrous acetone containing 2% osmium tetroxide. The samples were kept in the freeze-substitution medium at -90° C, -60° C and -30° C for 8 hours at each temperature step (Müller et al., 1980). They were then washed in anhydrous acetone at -30° C and transfered to a critical point dryer (Balzers, FL) in which the acetone was replaced by liquid CO_2 at a temperature below +10° C. The specimens were then critical point dried.

Chemical fixation and dehydration: T4 polyheads were incubated for 2 hours with 2% glutaraldehyde at 4° C (the pH was adjusted to 7.2 with 0.1 M K_2CO_3). After fixation, the specimens were washed with bidistilled water and dehydrated at 4° C through a 30, 60, 90 and 100% ethanol series (10 minutes in each step). Ethanol was replaced by anhydrous acetone which was subsequently displaced by liquid CO_2 at a temperature below +10° C, prior to critical point drying.

Metal coating procedures

Unidirectional platinum/carbon shadowing for TEM: T4 polyheads were unidirectionally shadowed with platinum/carbon in a Balzers BAF 300 freeze-fracture device at an angle of 28°. The platinum/carbon layer (1.7 nm) was subsequently backed with approximately 20 nm of carbon evaporated perpendicular to the specimen (Buhle et al., 1985). The specimens were kept at -85° C at a pressure < 5 x 10^{-7} mbar during coating. Chemically fixed samples were cooled down to -85° C prior to coating.

Chromium double-axis rotary shadowing (DARS) for SEM: Chromium was electron beam evaporated in a Balzers BAF 300 freeze-fracture device at a pressure < 5 x 10^{-7} mbar at -85° C. DARS with a gun tilt range of 0° to 90°, was employed for this purpose. The thickness of the metal films was 6 nm, measured by a quartz crystal monitor moving on target with the electron gun. The resulting metal layer is not homogeneous in thickness; increasing from 1/5th, on vertical surfaces, to 2/3rds of the measured thickness on horizontal surface planes (according to model calculations, Hermann et al., 1988; Hermann and Müller, 1991).

Low temperature planar magnetron sputtering (PMS) for SEM: Chromium was PMS

deposited in a Balzers MED 010 table top high vacuum coating device. The normal glass recipient was replaced by an aluminum cylinder adapted for low temperature work. The modified recipient contains a port through which the Gatan cold stage can be inserted, and a LN_2 cooled Meissner trap with vacant orifices for the quartz crystal and for the specimen on the cold stage (Müller and Hermann, 1990; Hermann and Müller, 1991). Immediately after freezing, specimens were mounted on the cryoholder under liquid nitrogen and introduced into the PMS device with the cryoshield of the cryoholder closed. The cryoholder was inserted against a slow flow of dry nitrogen gas in order to reduce contamination of the cold trap. The cryoshield of the cryoholder was opened after a pressure < 10^{-6} mbar was attained; the temperature was then increased to -85° C for freeze-drying. The pressure was reduced prior to sputtering to 5 x 10^{-2} mbar by introduction of pure argon gas. Sputtering was carried out at a substrate to target distance of 7.5 cm. The sample was cooled to -150° C prior to venting with dry nitrogen gas and immediately transferred to the microscope under liquid nitrogen using the conventional Gatan cryostation (the modified recipient, HR 010, is now available from Balzers, FL).

Electron microscopy

A Hitachi H-600 was used for TEM study. The SEM samples were examined in a Hitachi S-900 in-lens field-emission scanning electron microscope on a Gatan cryoholder at approx. -80° C. The microscope is equipped with an improved YAG type BSE detector (Autrata et al., 1986; Autrata et al., 1991; available from Plano GmbH, Marburg, Germany). Specimen areas were preselected during high speed scans at low magnification (10,000 x). Micrographs were then taken immediately at 200,000 x and final focussing was performed during the first lines of the exposure (2000 lines/80 sec total exposure).

Results

Freeze-drying of T4 polyheads preserved polyhead substructures (Fig. 1B), while structural details were completely lost after glutaraldehyde fixation followed by dehydration and critical point drying (Fig. 1A).

Critical point drying after freeze-substitution in acetone containing 2% osmium tetroxide resulted in pure structural definition, as demonstrated in figure 1C. Identically freeze-substituted polyheads, but freeze-dried from acetone at -100° C permitted identification of polyhead substructures (Fig. 1D).

Chromium coated test specimens yielded high resolution structural information only during the first scan of the electron beam if photographed at high magnifications and ambient temperature in the SEM (at a scanspeed of 80 seconds per 2000 lines; Fig. 2A). The second scan over the same area already causes severe loss of structural information (Fig. 2B). Cooling the specimen to -80° C permits 3 to 4 scans without loss of structural information (Fig. 2C, first and, Fig. 2D, second scan over the same area).

High acceleration voltage yielded the best results of both, SE imaging and BSE detection. Freeze-dried and chromium coated samples (of T4 polyheads and of Fab fragments coupled to 0.8 nm gold colloids) were observed at a magnification of 200,000 fold under conditions of minimum contamination. SE images of T4 polyheads at different acceleration voltages are seen in figure 3. SE and BSE images of Fab fragments coupled to 0.8 nm colloidal gold at the same acceleration voltages are shown in figure 4.

Polyhead capsomere subunits and Fab fragments appear clear and crisp at an acceleration voltage of 30 kV (Fig. 3A and 4A), or 20 kV (not shown). The same structures are shown in figures 3B and 4C at an acceleration voltage of 7 kV. Fine structures are still visible, the shapes are, however, less distinct. The fine structures appear blurred in figures 3C and 4E which were taken at an acceleration voltage of 5 kV.

A large number of crisp colloidal gold particles is visible in figure 4B, a BSE image of gold marked Fab fragments at an acceleration voltage of 30 kV. The BSE signal increases, when the acceleration voltage is reduced to 7 kV, as shown in figure 4D. Gold particles appear larger than at 30 kV. The number of visible colloidal gold particles is reduced at 5 kV (Fig. 4F). Only larger clusters are detected.

Discussion

Freeze-drying of rapidly frozen samples preserves T4 polyhead substructures (Fig. 1B). Conventional chemical fixation and follow up procedures result, however, in loss of fine

Fig. 1: TEM micrographs (100 kV acceleration voltage) of unidirectionally platinum/carbon coated T4 polyheads.
Fig. 1A Chemically fixed and dehydrated polyheads after critical point drying. Not even the shape of the T4 polyheads is properly maintained.
Fig. 1B T4 polyheads, rapidly frozen and freeze-dried (-85° C). Polyhead capsomeres and their substructures are clearly visible.
Fig. 1C Polyheads freeze-substituted in anhydrous acetone containing 2% osmium tetroxide and subsequently critical point dried. Polyhead capsomeres are invisible.
Fig. 1D Identically freeze-substituted polyheads, but freeze-dried at -100° C from pure acetone. The capsomere structures are now visible.

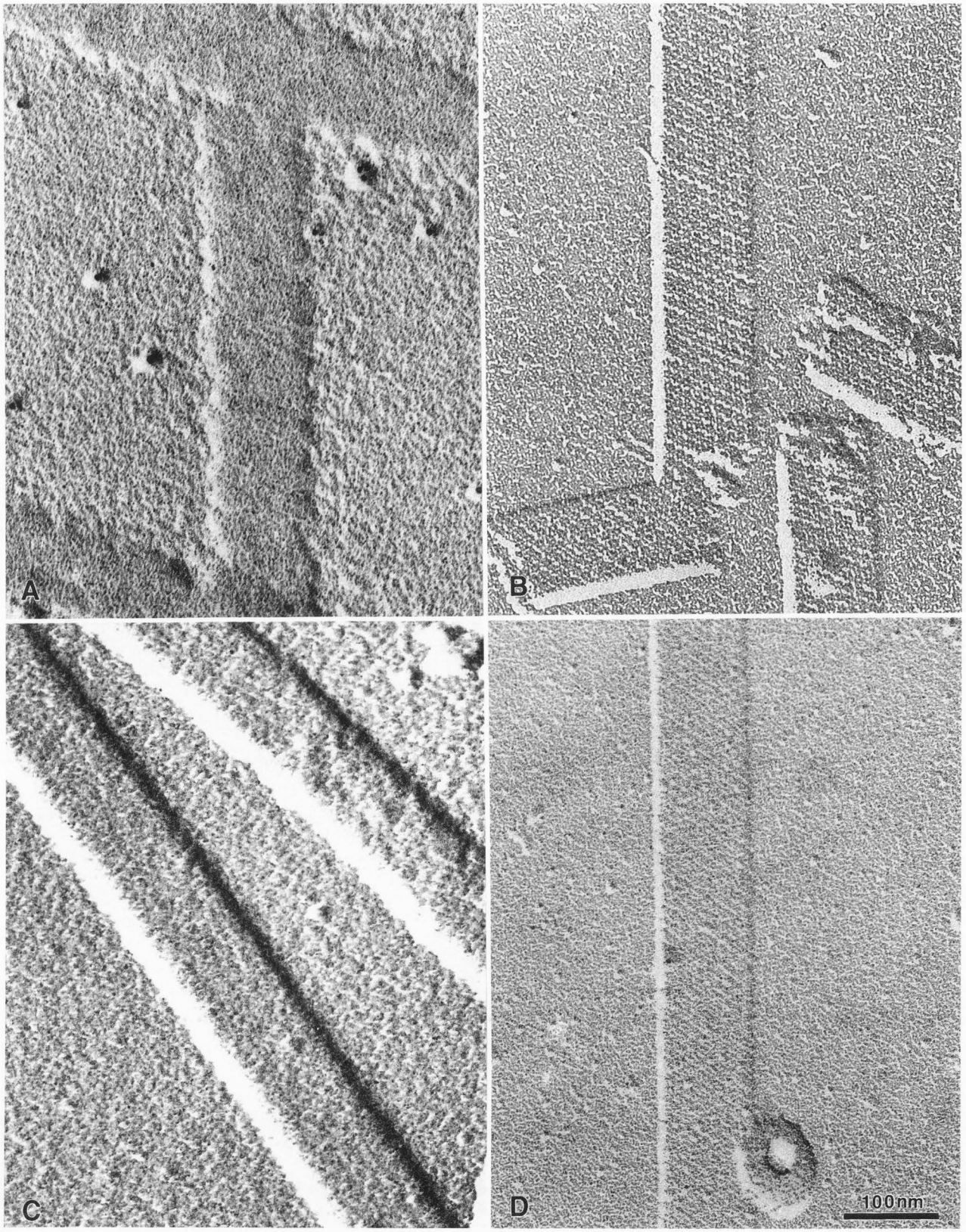
A
B
C
D
100nm

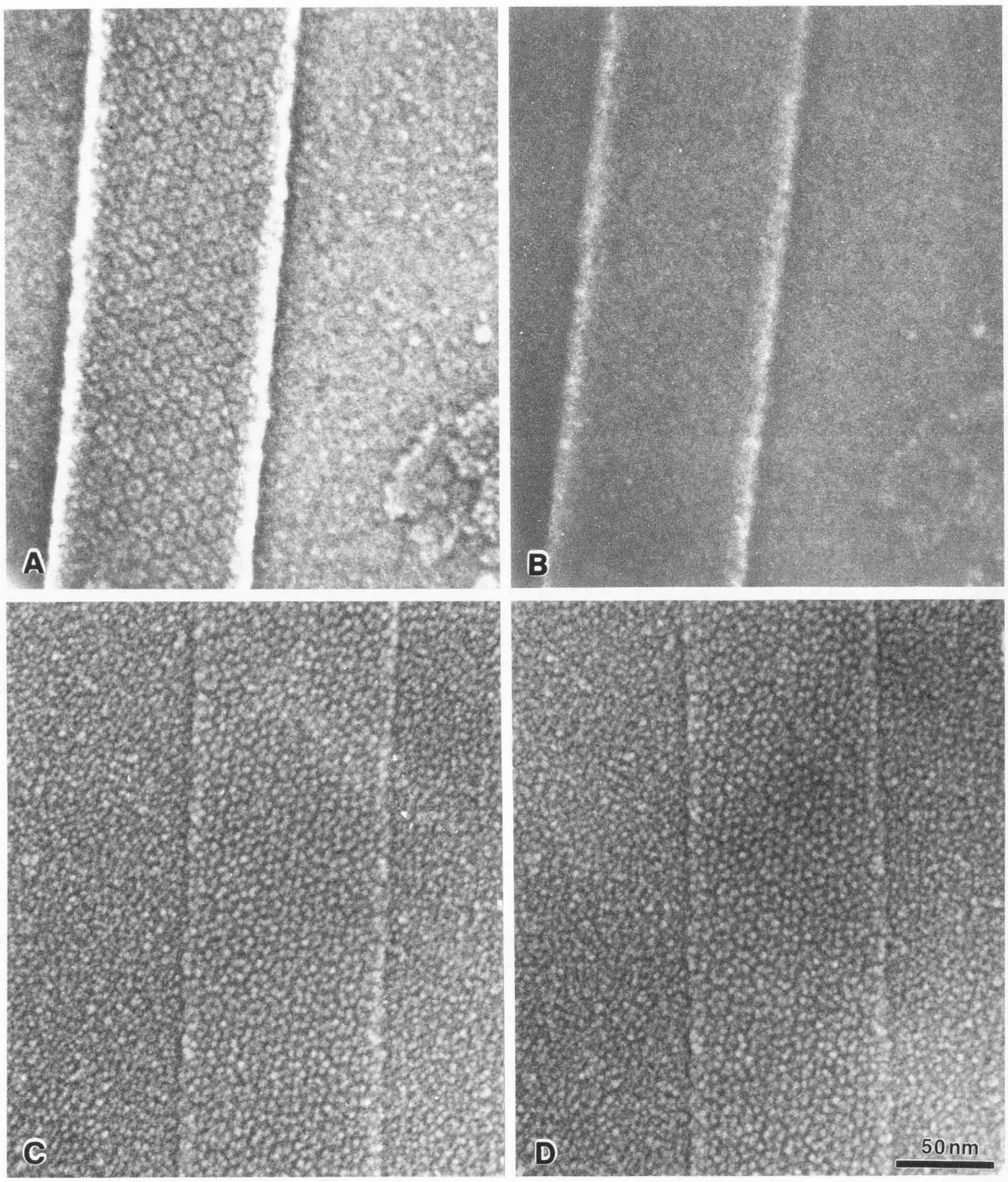

Fig. 2 demonstrates the importance of specimen cooling during observation in the SEM in order to minimize etching and contamination. **Fig. 2A** and **B** depict the same area of a freeze-dried and DARS chromium coated specimen kept at room temperature during the first and second scan of the electron beam (scanning speed 80 sec/2000 lines, acceleration voltage 30 kV).
Figs. 2C, D have been photographed during the first and second scan of the electron beam over the same specimen area after cooling the specimen to -80° C (freeze-dried, chromium planar magnetron sputtered specimens).

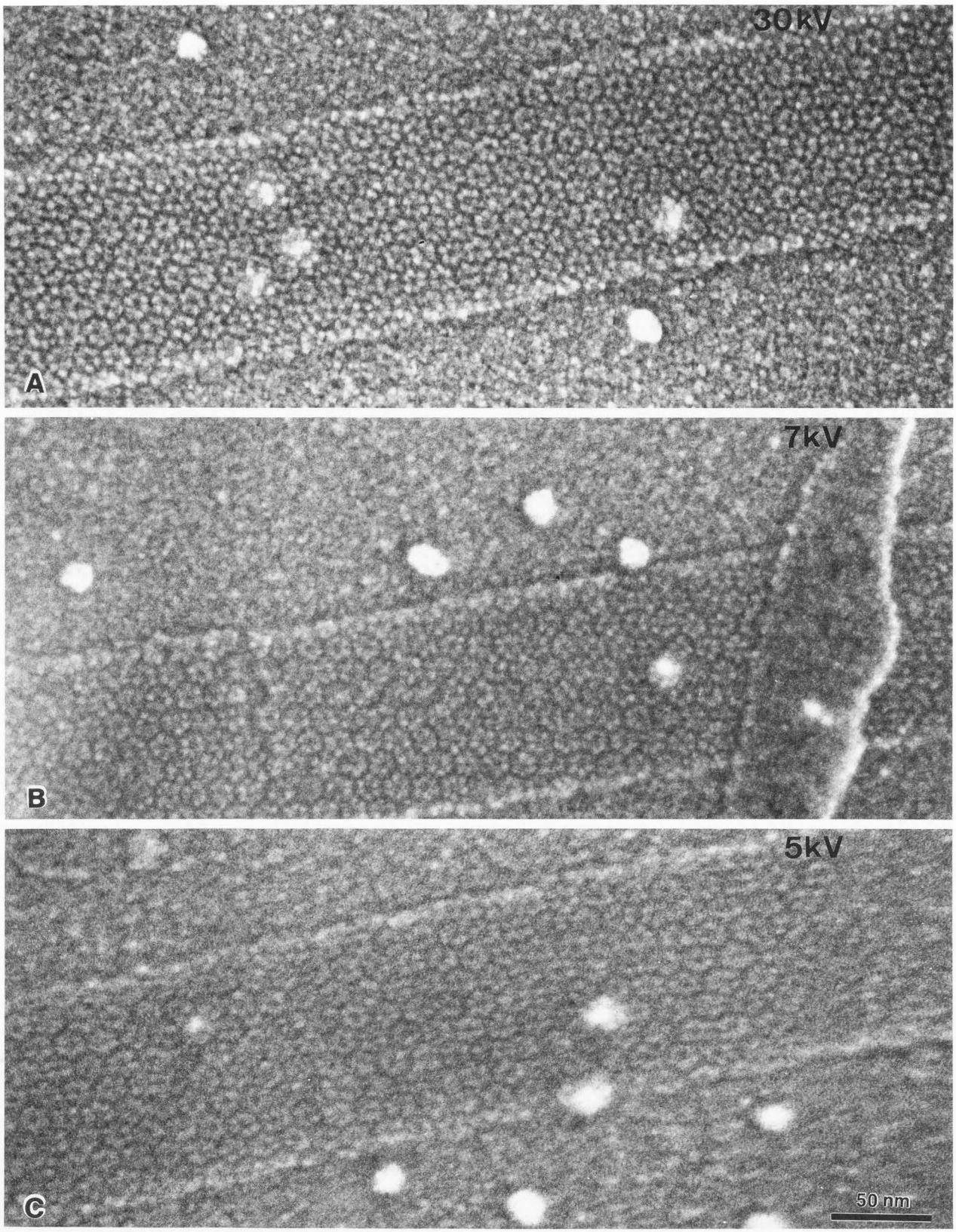

Fig. 3: SE images of freeze-dried, DARS chromium coated T4 polyheads at acceleration voltages of 30 kV (Fig. 3A), 7 kV (Fig. 3B) and 5 kV (Fig. 3C). Polyhead capsomeres and their substructures appear less crisp with decreasing acceleration voltage.

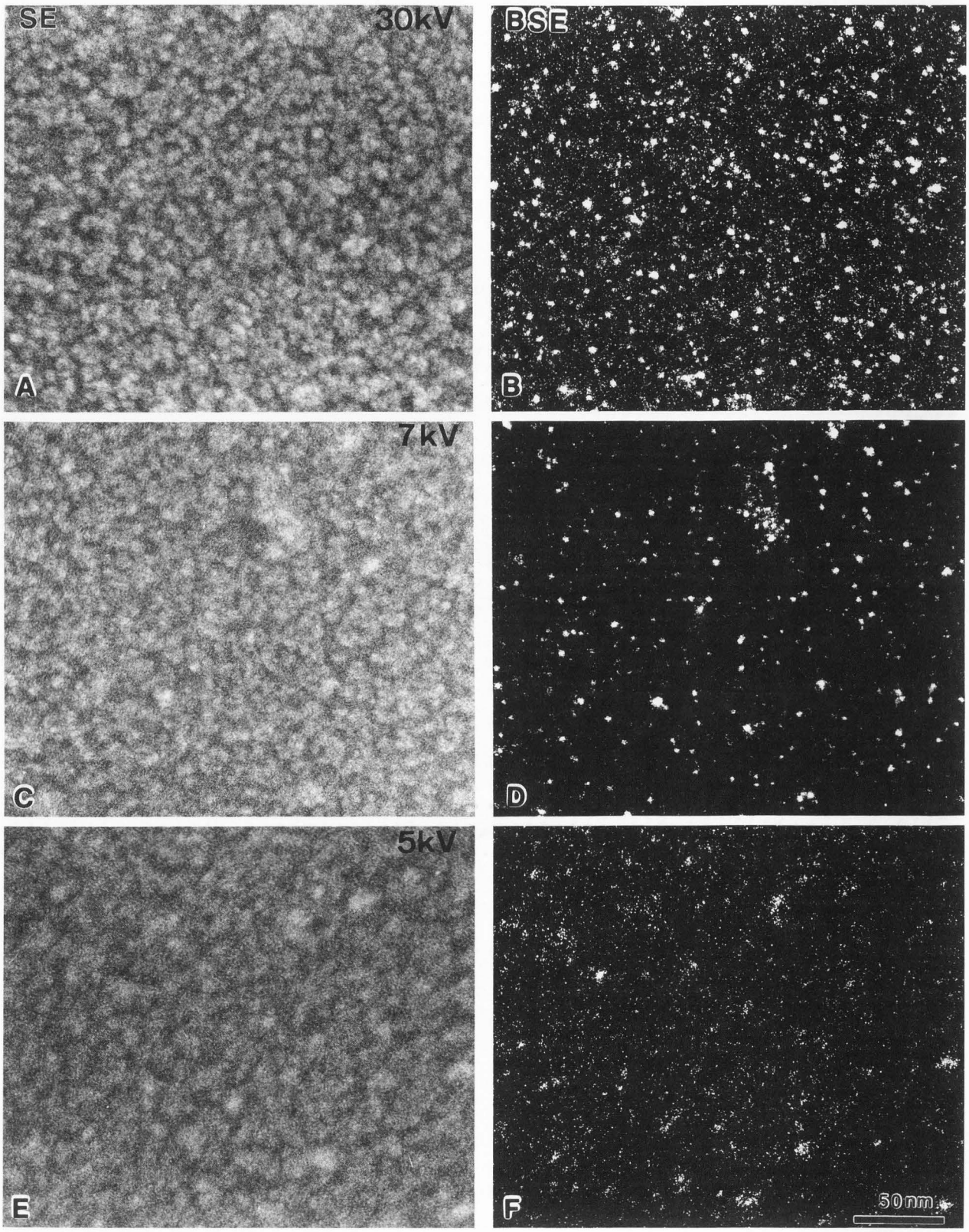
SE
30kV
A
BSE
B
7kV
C
D
5kV
E
F
50nm

Fig. 4 shows SE and BSE images of Fab fragments coupled to 0.8 nm colloidal gold at different acceleration voltages. The samples have been freeze-dried and DARS chromium coated at -85° C.

Figs. 4A, C, E are SE images of marked Fab fragments at an acceleration voltage of 30, 7 and 5 kV, while **Figs. 4B, D, F** depict the corresponding BSE images.

A large number of crisp colloidal gold particles is imaged at 30 kV (**Fig. 4B**). Individual gold particles and aggregates are readily discerned from the background noise (very small white points). The BSE signal increases at 7 kV, gold particles appear, however, larger than at 30 kV (**Fig. 4D**). At 5 kV, the individual gold particles are no longer clearly imaged (**Fig. 4F**); only larger particles are visible.

---

structural details (Fig. 1A). Glutaraldehyde fixation itself does not seem to destroy polyhead substructures. The capsomeres are readily identified after air-drying of glutaraldehyde fixed polyheads (not shown); air-drying of chemically untreated polyheads renders the capsomeres invisible (Kessel et al., 1986).

Unlike T4 polyheads, most biological samples can not be freeze-dried from bidistilled water due to their osmotic sensitivity. "Volatile buffers", e.g. ammoniumacetate or bicarbonate, do not sublime at temperatures below -35° C. This was determined by residual gas analysis in a Balzers BA 500 K ultra-high vacuum freeze-fracture device (A. Gisel, ETH Zürich, personal communication). The temperature dependent degree of dehydration at which biological structures of molecular dimensions are altered or lost during freeze-drying is not known. The relatively high collapse temperature of ovalbumin, -10° C, during freeze-drying (MacKenzie, 1972) suggests however, that it might be possible to warm biological samples to subzero temperatures at which volatile buffers sublime, without removing the water fraction necessary for maintaining structural integrity.

Freeze-drying of freeze-substituted samples renders polyhead capsomeres slightly visible (Fig. 1D). Structural details > 10 nm could be preserved by critical point drying of freeze-substituted biological specimens observed in SEM (Osumi et al., 1988; Walther and Hentschel, 1989). The polyhead capsomeres (8.3 nm in diameter) were no longer visible, however after freeze-substitution followed by critical point drying (Fig. 1C). The loss of structural information of freeze-substituted and critical point dried polyheads may be due to the use of solvents at relatively high temperatures; exchange of acetone with CO_2 was performed at temperatures below + 10° C. Protein molecules may collapse due to complete dehydration under these conditions (MacKenzie, 1972). Freeze-substituted polyheads were kept at temperatures below -30° C during the preparation steps of freeze-drying. The strong anisotropic shrinkage that can occur during critical point drying itself may also have influenced structural preservation (Boyde and Franc, 1981).

The metal coating procedure can limit structural resolution in the SEM. It has been optimized in a previous study on high resolution biological metal coating techniques (Hermann and Müller, 1991). The thickness and grain structure of the metal film influences the signal generation in the SEM. A high resolution SE signal is achieved by coating the specimen with chromium at -85° C. The optimal metal film thickness should be evaluated in a coating thickness series and does not necessarily correspond with the minimal thickness at which the metal grains coalesce.

The shape and size of fine structures is accurately visualized in the SE image only at high acceleration voltage (Figs. 3A and 4A). Fine structures appear blurred with reduced acceleration voltage (Figs. 3C and 4E). This study uses thin, beam-transparent samples, thus reducing the difficulties encountered with thicker specimens, i.e. charging and a larger SE II background signal. The level of structural information of the SE image may be reduced on bulk specimens. Detection of small colloidal gold particles with the BSE image is possible, however, on bulk biological samples; 1 nm gold particles can be unambiguously localized on surfaces of erythrocytes at an acceleration voltage of 30 kV (Müller and Hermann, 1990). Colloidal gold particles appear crisp at an acceleration voltage of 30 kV in the BSE image (Fig. 4B), but "larger than life" at an acceleration voltage of 7 kV (Fig. 4D). Dimensions close to the resolution limit of the microscope are, however, difficult to measure. The number of visible gold particles decreases significantly when the acceleration voltage is further reduced (Fig. 4F). The corresponding SE image (Fig. 4E) indicates that the number of structures does not differ significantly from figure 4A, taken at 30 kV. This indicates that the reduced number of gold particles in figure 4F is due to the acceleration voltage rather than to an uneven distribution of the labelled Fab fragments on the support.

The observed loss of information in SE (Figs. 3) and BSE images (Fig. 4B, D, F), at an acceleration voltage below approximately 7 kV, corresponds to calculations of beam size diameter of the Hitachi S-900 SEM as a function of the acceleration voltage (Nagatani et al., 1987; estimation by wave optics).

Conclusions

Adequate structural preservation is maintained only when the biological specimen can be

kept in a controlled state of hydration during metal coating and subsequent observation in the SEM.

High precision localization of surface structures should be performed at high acceleration voltage. This is also true for unambiguous detection of ultra-small colloidal gold markers (ca. 1 nm) by backscattered electrons in SEM immunolabelling studies (Hermann et al., 1991).

Acknowledgements

We thank M. I. Yaffee for his help with the manuscript. T4 polyheads were kindly provided by Prof. U. Aebi, Biozentrum Basel; Fab fragments were supplied by H. Schwarz, Max-Planck-Institut für Biologie, Tübingen.

References

Autrata R, Hermann R, Müller M (1991). An efficient BSE single crystal detector for SEM. Scanning, in press.

Autrata R, Walther P, Kriz S, Müller M (1986). A BSE scintillation detector in the (S)TEM. Scanning; 8: 3 - 8.

Baba M, Osumi M (1987). Transmission and scanning electron microscopic examination of intracellular organelles in freeze-substituted *Kloeckera* and *Saccharomyces cerevisiae* yeast cells. J. Electron Micr. Techn.; 5: 249 - 261.

Barlow DI, Sleigh MA (1979). Freeze substitution for preservation of ciliated surfaces for scanning electron microscopy. J. Microsc. (Oxford); 115: 81 - 95.

Beckett A, Read ND (1986). Low-temperature scanning electron microscopy. In: Aldrich HC, Todd WJ (eds.): Ultrastructural techniques for microorganisms. Plenum Press, New York, London: 45 - 86.

Boyde A, Franc F (1981). Freeze-drying shrinkage of glutaraldehyde fixed liver. J. Microsc.; 122: 75 - 86.

Bridgman PC, Reese TS (1984). The structure of cytoplasma in directly frozen cultured cells. I. Filamentous meshworks and the cytoplasmic ground substance. J. Cell Biol.; 99: 1655 - 1668.

Buhle EL Jr., Aebi U, Smith (1985). Correlation of surface topography of metal-shadowed specimens with their negatively stained reconstructions. Ultramicroscopy; 16: 436 - 450.

Coetzee J, Van der Merwe CF (1984). Extraction of substances during glutaraldehyde fixation of plant cells. J. Microsc.; 135: 147 - 158.

DeRosier DJ, Klug A (1972). Structure of the tubular variants of the head of bacteriophage T4 (polyheads). I. Arrangement of subunits in some classes of polyheads. J. Mol. Biol.; 65: 469 - 488.

Engel A (1981). Beam damage contamination and etching. In: Jouffrey B., Bourret A., Colliex C. (eds.): Éditions du CNRS, Microscopie électronique en science des materiaux: 185 - 192.

Finch JT, Klug A, Stretton AOW (1964). The structure of the polyheads of T4 bacteriophage. J. Mol. Biol.; 10: 570 - 575.

Fourie JT (1976). Contamination phenomena in cryopumped TEM and ultra-high vacuum field-emission STEM system. Scanning Electron Microsc.; 1976; I: 53 - 60.

Gross H, Müller T, Wildhaber I, Winkler H (1985). High resolution metal replication, quantified by image processing of periodic test specimens. Ultramicroscopy; 16: 287 - 304.

Hermann R, Müller M (1991). High resolution biological scanning electron microscopy: A comparative study of low temperature metal coating techniques. J. Electron Microsc. Techn.; in press.

Hermann R, Pawley J, Nagatani T, Müller M (1988). Double-axis rotary shadowing for high-resolution scanning electron microscopy. Scanning Microsc.; 2: 1215 - 1230.

Hermann R., Schwarz H., Müller M. (1991). High precision immuno scanning electron microscopy using Fab fragments coupled to ultra-small colloidal gold. J. Struct. Biol.; in press.

Hodges G.M., Southgate J., Toulson E.C. (1987). Colloidal gold - a powerful tool in scanning electron microscope immunocytochemistry: an overview of bioapplications. Scanning Microsc.; I: 301 - 318.

Horisberger M, Rosset J (1977). Colloidal gold, a useful marker for transmission and scanning electron microscopy. J. Histochem. Cytochem., 25: 295 - 305.

Hren JJ (1979). Barriers to AEM: Contamination and etching. In: Hren JJ, Goldstein J, Joy DC Plenum Press, New York, London, Introduction to analytical EM; 481 - 505.

Hülser DF, Paschke D, Greule J (1989). Gap junctions: correlated electrophysiological recordings and ultrastructural analysis by fast freezing and freeze-fracturing. In: Plattner H (ed.): Electron microscopy of subcellular dynamics. CRC Press, Inc., Boca Raton, Florida: 33 - 49.

Joy DC (1984). Monte Carlo studies of high-resolution secondary imaging. Microbeam Analysis; 1984: 81 - 86.

Kessel M, Buhle EL Jr., Glavaris E, Aebi U (1986). A novel method for preventing collapse of air-dried specimens for heavy metal shadowing. Proc. 44th Ann. Meet. Electr. Microsc. Soc. Am.; 228 - 229.

Kiss JZ, Giddings TH Jr., Staehelin LA, Sack FD (1990). Comparison of the ultrastructure of conventionally fixed and high pressure frozen/freeze substituted root tips of *Nicotiana* and *Arabidopsis*. Protoplasma; 157: 64 - 74.

Kistler J, Aebi U, Onorato L, Ten Heggeler B, Showe MK (1978). Structural changes during

the transformation of bacteriophage T4 polyheads: characterization of the initial states by freeze-drying and shadowing Fab-fragment-labelled preparations. J. Mol. Biol.; 126: 571 - 589.

Knoll G, Plattner H (1989). Ultrastructural analysis of biological membrane fusion and a tentative correlation with biochemical and biophysical aspects. In: Plattner H (ed.): Electron microscopy of subcellular dynamics. CRC Press, Inc., Boca Raton, Florida: 95 - 117.

Knoll G, Verkleij AJ, Plattner H (1987). Cryofixation of dynamic processes in cells and organelles. In: Steinbrecht RA, Zierold K (eds.): Cryotechniques in biological electron microscopy. Springer Verlag, Berlin, Heidelberg: 258 - 271.

Laemmli UK, Amos LA, Klug A (1976). Correlation between structural transformation and cleavage of the major head protein of T4 bacteriophage. Cell; 7: 191 - 203.

Lee RMKW (1984). A critical appraisal of the effects of fixation, dehydration and embedding on cell volume. In: Revel J-P, Barnard T. Haggis GH (eds.): The science of biological specimen preparation. SEM Inc, AMF O'Hare, Chicago, IL 60666: 61 - 70.

MacKenzie AP (1972). Freezing, freeze-drying, and freeze-substitution. Scanning Electron Microsc.; 1972; II: 273 - 280.

Miller KR, Prescott CS, Jacobs TL, Lassignel NC (1983). Artifacts associated with quench-freezing and freeze-drying. J. Ultrastruct. Res.; 82: 123 - 133.

Moor H (1987). Theory and practice of high pressure freezing. In: Steinbrecht RA, Zierold K (eds.): Cryotechniques in biological electron microscopy. Berlin, Springer: 175-191

Müller M, Hermann R (1990). Towards high resolution SEM of biological objects. In: Peachy LD. Williams DB (eds.): San Francisco Press, San Francisco, Proc. XIIth Int. Congr. Electron Microsc.; 3: 4 - 5.

Müller M., Marti T., Kriz S.R. (1980). Improved structural preservation by freeze substitution. In: Brederoo P, de Priester W (eds.): Proc. 7th Eur. Congr. Electron Microsc. II: 720 - 721.

Müller M, Moor H (1984). Cryofixation of suspensions and tissues by propane-jet freezing and high-pressure freezing. Proc. 42nd Ann. Meet. Electron Microsc. Soc. Am.; 6 - 9.

Müller M, Walther P, Hermann R, Schwarb P (1989). SEM-immunocytochemistry with small (5 - 15 nm) colloidal gold markers. In: Verkleij A.J., Leunissen J.L.M. (eds.): Immuno-gold labeling in cell biology. CRC Press, Inc., Boca Raton, Florida: 199 - 216.

Nagatani T, Saito S, Sato M, Yamada M (1987). Development of an ultrahigh resolution scanning electron microscope by means of a field emission source and in-lens system. Scanning Microsc.; 1: 901 - 909.

Osumi M, Baba M, Naito N, Taki A, Yamada N, Nagatani T (1988). High resolution, low voltage scanning electron microscopy of uncoated yeast cells fixed by the freeze-substitution method. J. Electron Microsc.; 37: 17 - 30.

Peters K-R (1982). Conditions required for high quality high magnification images in secondary electron-I scanning electron microscopy. Scanning Electron Microsc. 1982; IV: 1359 - 1372.

Peters K-R (1986). Metal deposition by high-energy sputtering for high magnification electron microscopy. In: Koehler JK, ed.: Advanced techniques in biological electron microscopy III, Springer Verlag, Berlin: 101 - 166.

Porter RR (1959). The hydrolysis of rabbit g-globulin and antibodies with crystalline papain. Biochem. J.; 73: 119 - 127.

Read ND, Jeffree CE (1991). Low-temperature scanning electron microscopy in biology. J. Microsc.; 161: 59 - 72.

Sato F, Nakaizumi Y., Yamada M, Nagatani T (1990). Development of a low accelerating voltage SEM (S-900H), Hitachi Instrument News; 19: 45 - 49.

Slot JW, Geuze HJ (1985). A new method of preparing gold probes for multiple-labeling cytochemistry. E. J. Cell Biol.; 38: 87 - 93.

Studer D, Michel M, Müller M (1989). High pressure freezing comes of age. Scanning Microsc. suppl.; 3: 253 - 269.

Wall JS (1980). Contamination in the STEM at ultra high vacuum. Scanning Electron Microsc. 1980; I: 99 - 106.

Walther P, Ariano BH, Kriz SR, and Müller M (1983) High resolution SEM detection of protein-A gold (15 nm) marked surface antigens using backscattered electrons. Beitr. Elektronenmikroskop. Direktabb. Oberfl., 16: 539 - 545.

Walther P, Hentschel J (1989). Improved representation of cell surface structures by freeze substitution and backscattered electron imaging. Scanning Microsc. Suppl.; 3: 201 - 211.

Walther P, Hentschel J Herter P, Müller T, Zierold K (1990). Imaging of intramembraneous particles in frozen-hydrated cells (*Saccharomyces cerevisiae*) by high resolution cryo-SEM. Scanning; 12: 300 - 307.

Walther P, Hentschel J, Scott D (1988). Improved method for the identification of cell surface structures in field emission SEM: a combination of fast freezing, freeze substitution and critical point drying. Inst. Phys. Conf. Ser. No. 93; 3: 49 - 50.

Walther P, Müller M (1986). Detection of small (5 - 15 nm) gold-labelled surface antigens using backscattered electrons. In: The science of biological specimen preparation, SEM Inc., AMF O'Hare, (Chicago), IL 60666, USA: 195 - 201.

Walther P, Müller M, Schweingruber ME (1984). The ultrastructure of the cell surface and plasma membrane of exponential and stationary phase cells of *Schizosaccharaomyces pombe*, grown in different media. Arch. Microbiol.; 137: 128 - 134.

Discussion with reviewers

K.R. Peters: The usefulness of chromium and high accelerating voltage for field-emission SEM imaging of high magnification details for thin TEM samples is in agreement with similar imaging reports of surface detail on bulk samples with strong mass density depth variations as found in osmificated cellular or tissue samples. Why do you have to use a much larger amount of metal for contrast production on your thin samples as you do not have to override contrast contributions from the background signal?
Authors: The thickness of the coating layer must be optimized for maximum contrast (Hermann and Müller, 1991). This thickness depends not only on the coating procedure, technique and material, but also on the type of specimen (bulk or TEM-like as in this paper) and on the attainable resolution (magnification). Data drawn from different sources (i.e. other techniques, samples and/or, follow-up procedures) therefore do not provide adequate basis for comparison of coating parameters.

K. Zierold: Can the radiation damage you show in Fig. 2 be reduced by use of another coating material, for example platinum?
Authors: The influence of different coating materials (we examined Cr, Ge, Pt, Pt/C, W) is minimal compared to the effects of the low temperature.

K. Zierold: Why does colloidal gold appear fuzzy and irregularly shaped in SEM in comparison to the sharp round circles seen in TEM?
Authors: 0.8 nm colloidal gold particles consist of less than 20 atoms and are about the size of the scanning electron beam. Therefore only a very noisy signal can be expected.

1 nm colloidal gold particles appear also fuzzy in TEM and are difficult to distinguish from noise. 10 or 15 nm colloidal gold particles are visualized in SEM with crisp, sharp contours (see Hermann et al., 1988).

K.R. Peters: The removal of water from frozen hydrated specimens may produce collapse at a macromolecular level in dependence of the elasticity of the molecular matrix. One factor altering the elasticity is the specimen temperature. How do you describe the imaging history of frozen and partially or fully hydrated sample surfaces in regard of macromolecular collapse?
K. Zierold: Does the macromolecular structure also collapse after freeze-drying, coating and warming up to room temperature or after freeze-drying and coating at room temperature? In other words: Could you comment on the critical temperature the specimen should not exceed before cryo SEM?
Authors: We don't think that there are reliable and conclusive data available yet to qualify as an answer to the above questions. There is, however, evidence accumulated in several reviews that only a minor portion of water can be removed from the specimen without structural consequences (see e.g. *Humbel BM, Müller M (1986). Freeze substitution and low temperature embedding. In: The science of biological specimen preparation 1985, SEM Inc., AMF O'Hare, (Chicago), IL 60666, USA: 175 - 183.* and *Kellenberger E (1991). The potential of cryofixation and freeze substitution: Observations and theoretical considerations. J. Microsc.; 161(2): 183 - 203.*).

As a rule of thumb, we assume that the specimen should never become warmer than -85° C, even with partially freeze-dried samples.

P. Walther: The level of structural information may be reduced on bulk samples, as explained in the discussion. Do you have any experimental evidence for this? Did you ever try to image the polyhead on a grid bar or on a bulk specimen support? Do you see a way to overcome these limitations?
Authors: The aim of our experiments was to evaluate the resolution limits of biological high resolution SEM. For this purpose we chose beam-transparent test specimens of known structure at molecular dimensions which contribute a minimum background signal. Several questions concerning thin samples are more readily studied with this type of SEM approach than with TEM.

Bulk samples provide a larger unspecific background signal which may obscure high resolution structural information. Several approaches to this problem have to be considered; among them, working at low voltages, BSE-imaging of unidirectionally shadowed surfaces, and SE I imaging at very high magnification.

P. Walther: Is the level of contamination shown in Fig. 2 influenced by the specimen support? Does it make a difference, whether pure carbon films, or carbon coated formvar films, or bulk carbon specimen supports are used?
Authors: The use of other beam-transparent support material, e.g. pure carbon films does not significantly influence contamination and etching. Little is known about these effects.